

Enhancing the electrocatalytic OER activity of Co-MOFs through labile solvents coordination

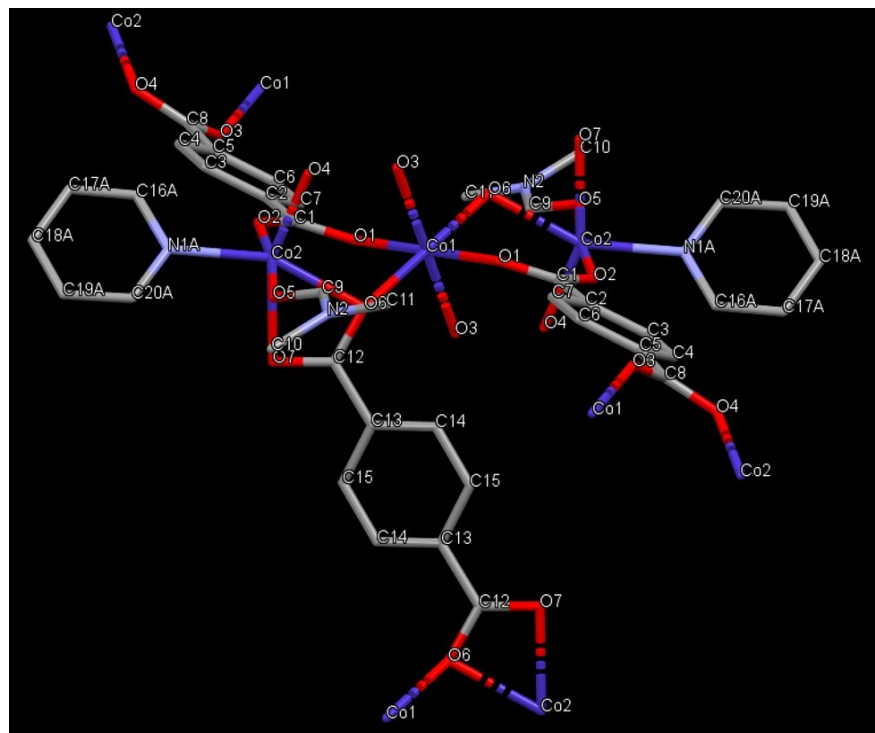


Figure S1. Molecular structure in the crystal lattice of **Co-MOF-1**. C (grey), H (white), N (blue), O (red) and Co (dark blue). Hydrogen atoms are removed for clarity.

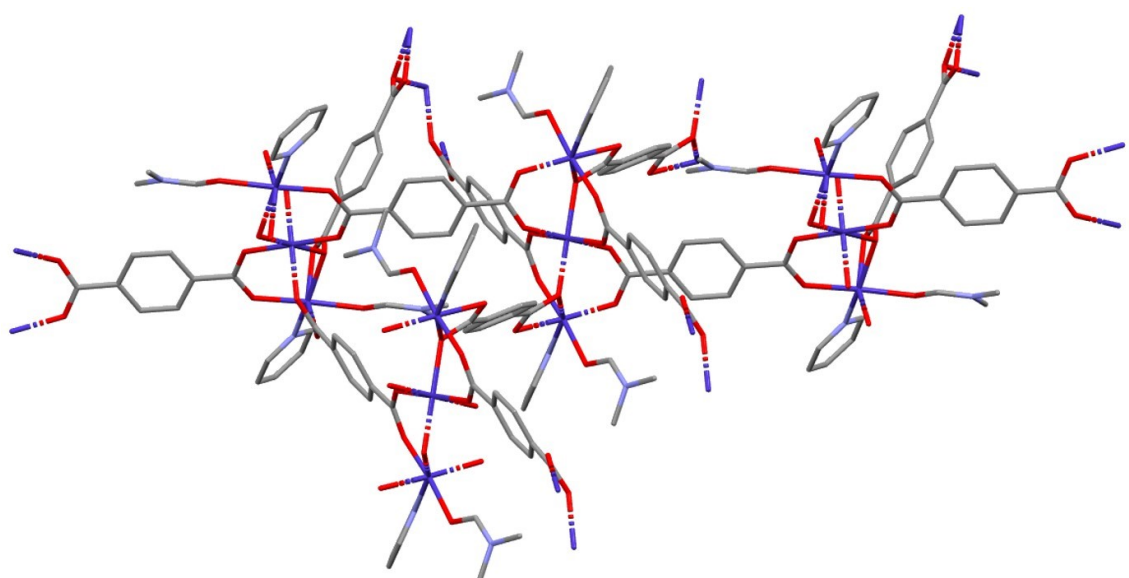


Figure S2. The coordination of BDC, pyridine and DMF with different cobalt centre of **Co-MOF-1**. C (grey), H (white), N (blue), O (red) and Co (dark blue). Hydrogen atoms are removed for clarity.

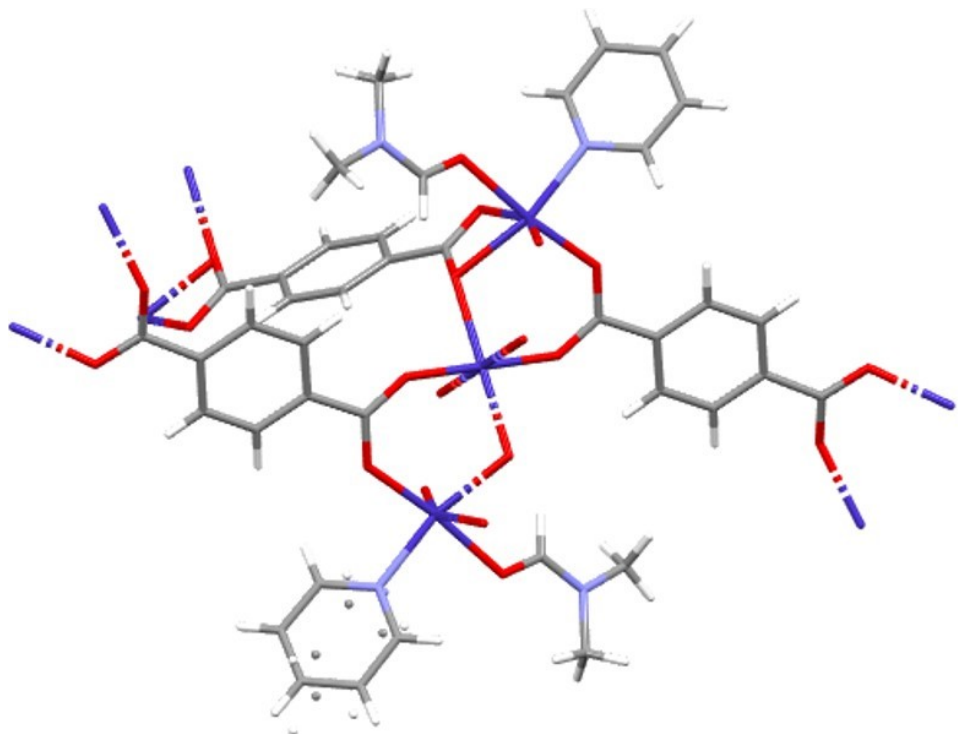


Figure S3. Molecular structure of **Co-MOF-1** in the crystal lattice. C (grey), H (white), N (blue), O (red) and Co (dark blue).

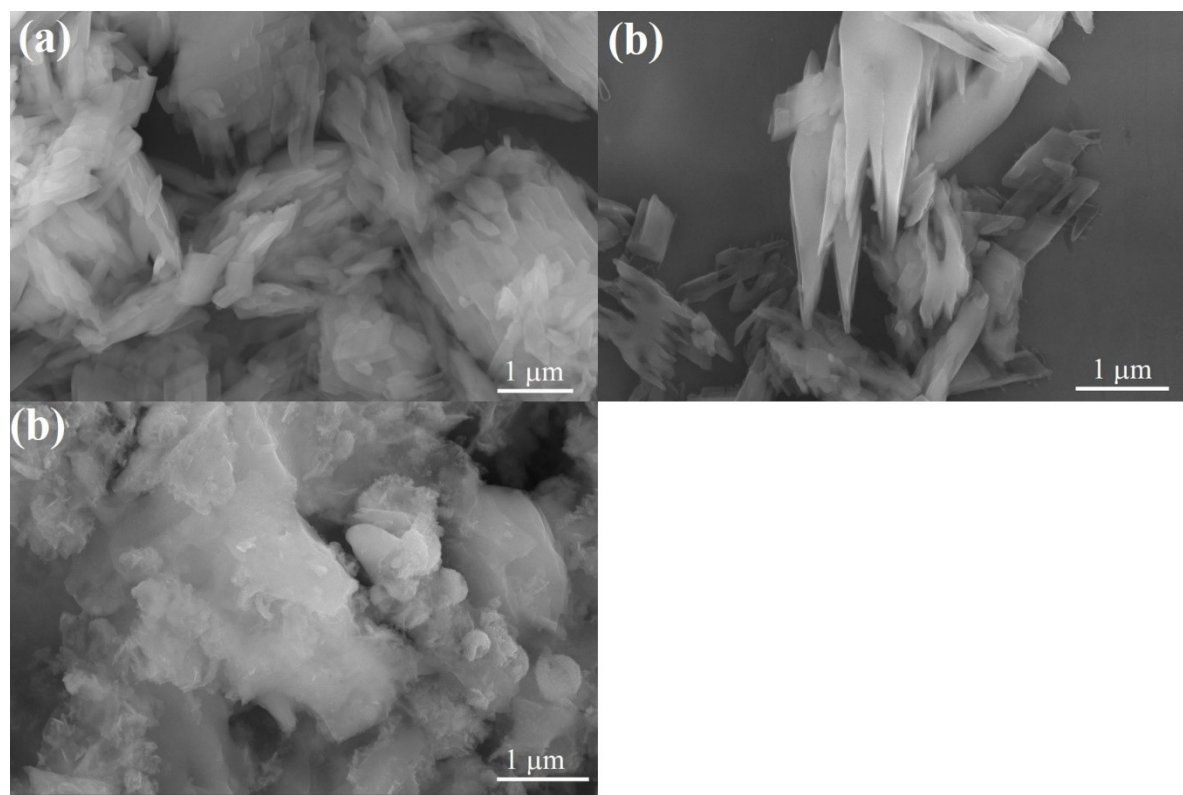


Figure S4. FE-SEM images of (a) **Co-MOF-1**, (b) **Co-MOF-2** and (c) **Co-MOF-1** (after catalysis)

Table S1. Crystal data and structure refinement for **Co-MOF-1** (CCDC No 2246026).

	Co-MOF-1
Identification code	
Empirical formula	C ₄₀ H ₃₆ Co ₃ N ₄ O ₁₄
Formula weight	973.52
Temperature	220(2) K
Wavelength	0.610 Å
Crystal system	Monoclinic
Space group	P2 ₁ /n
Unit cell dimensions	a = 14.496(3) Å α= 90°. b = 9.7410(19) Å β= 109.61(3)°. c = 16.453(3) Å γ = 90°.
Volume	2188.4(8) Å ³
Z	2
Density (calculated)	1.477 Mg/m ³
Absorption coefficient	0.782 mm ⁻¹
F(000)	994
Crystal size	0.105 x 0.065 x 0.020 mm ³
Theta range for data collection	1.393 to 24.999°.
Index ranges	-20<=h<=20, -13<=k<=13, -22<=l<=22
Reflections collected	21779
Independent reflections	6077 [R(int) = 0.0908]
Completeness to theta = 21.469°	99.3 %
Absorption correction	Empirical
Max. and min. transmission	1.000 and 0.862
Refinement method	Full-matrix least-squares on F ²
Data / restraints / parameters	6077 / 178 / 334
Goodness-of-fit on F ²	1.001
Final R indices [I>2sigma(I)]	R1 = 0.0662, wR2 = 0.1859
R indices (all data)	R1 = 0.0779, wR2 = 0.1934
Extinction coefficient	n/a
Largest diff. peak and hole	2.616 and -0.716 e.Å ⁻³

Table S2. Crystal data and structure refinement for **Co-MOF-2**.

	Co-MOF-2
Identification code	
Empirical formula	C38 H36 Co3 N2 O16
Formula weight	953.48
Temperature	220(2) K
Wavelength	0.630 Å
Crystal system	Monoclinic
Space group	C2/c
Unit cell dimensions	a = 33.257(7) Å b = 9.810(2) Å c = 17.964(4) Å
	α= 90°. β= 97.78(3)°. γ = 90°.
Volume	5807(2) Å ³
Z	4
Density (calculated)	1.091 Mg/m ³
Absorption coefficient	0.643 mm ⁻¹
F(000)	1948
Crystal size	0.125 x 0.058 x 0.015 mm ³
Theta range for data collection	1.096 to 26.495°.
Index ranges	-46<=h<=46, -12<=k<=12, -25<=l<=25
Reflections collected	24935
Independent reflections	7446 [R(int) = 0.1283]
Completeness to theta = 22.210°	98.9 %
Absorption correction	Empirical
Max. and min. transmission	1.000 and 0.799
Refinement method	Full-matrix least-squares on F ²
Data / restraints / parameters	7446 / 0 / 271
Goodness-of-fit on F ²	0.828
Final R indices [I>2sigma(I)]	R1 = 0.0816, wR2 = 0.2140
R indices (all data)	R1 = 0.1967, wR2 = 0.2381
Extinction coefficient	n/a
Largest diff. peak and hole	1.166 and -0.861 e.Å ⁻³

S. No	Catalyst	Org. linker	Substrate	Over potential η at 10mA	Tafel mV/dec	Reference
1	Ultrathin 2D Co-MOF	Terephthalate	GCE	371	74	1
2	CoBDC	Terephthalate	GCE	334	-	2
3	CoMONs	Terephthalate	Carbon paper	309	75.71	3
4	CoBDC-Fc-NF	Terephthalate and Ferrocene carboxylic acid	Nickel Foam	178	51	4
5	Ti ₃ C ₂ Tx–CoBDC	Citrate	GCE	410	48.2	5
6	Co-BPDC/Co BDC-3	1,4-benzenedicarboxylic acid and 4,4'-biphenyldicarboxylate	GCE	335	72.1	6
7	UTSA-16	Citrate	GCE	408	77	7
8	Co-MOF NF	Terephthalic acid	Nickel foam	311 @50mA	77	8
9	MAF-X27-OH	1H,5H-benzo(1,2-d:4,5-d')bistriazole	GCE	387	60	9
10	Co-OBA/C	4,4'-oxybis(benzoic acid), and imidazole	GCE	774 (vs Ag/AgCl)	85.7 (vs Ag/AgCl)	10
11	Co-MOF@CNTs (5 wt%)	benzimidazole	GCE	340	69	11
12	CoTPA-D	Terephthalate	Carbon cloth	273	67	12
13	Co-MOF-1	Terephthalate	GCE	294	57.5	This work

Table S3. Comparison of Co-MOFs electrocatalytic OER activity.

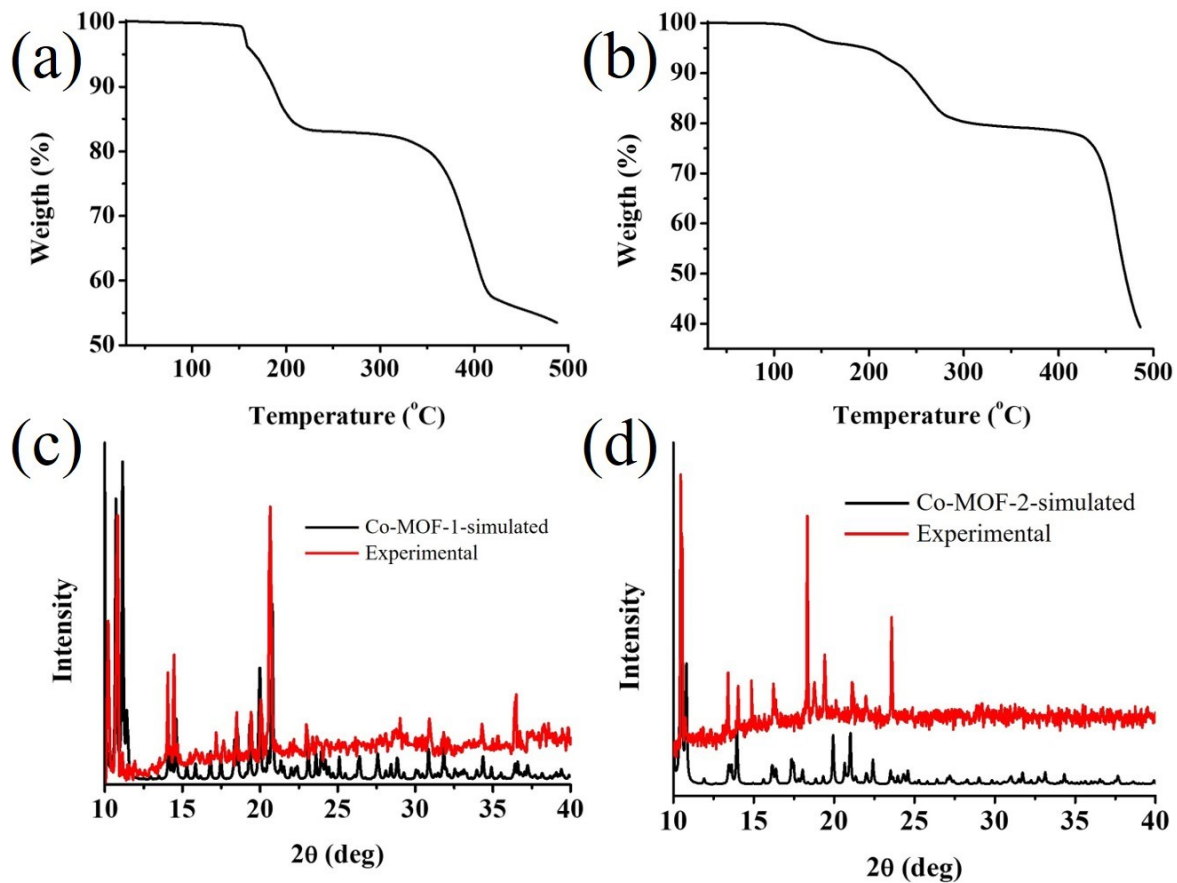


Figure S5. (a, b) PXRD and (c, d) TGA of (a, c) **Co-MOF-1** and (b, d) **Co-MOF-2**.

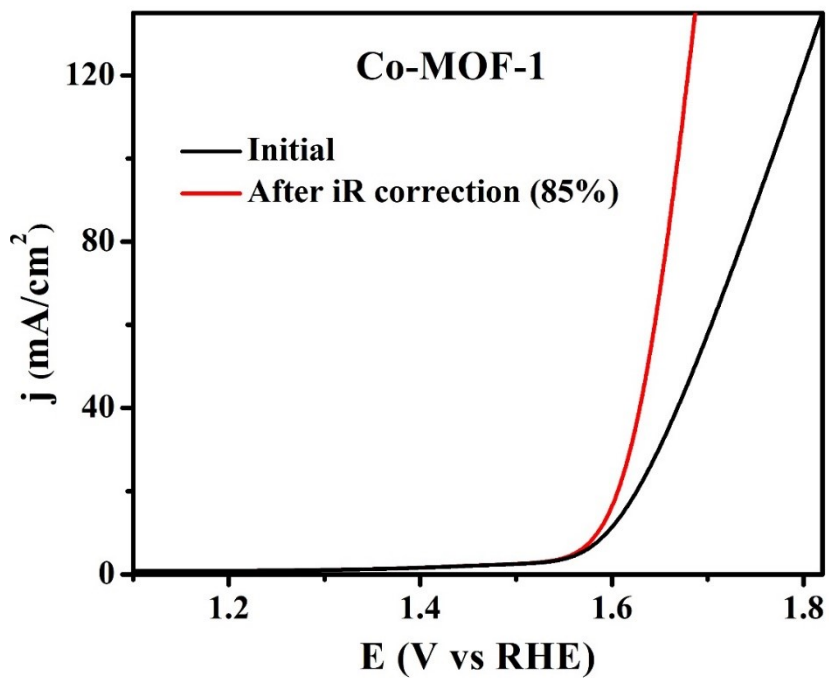


Figure S6. OER polarization curves of **Co-MOF-1** before and after iR correction.

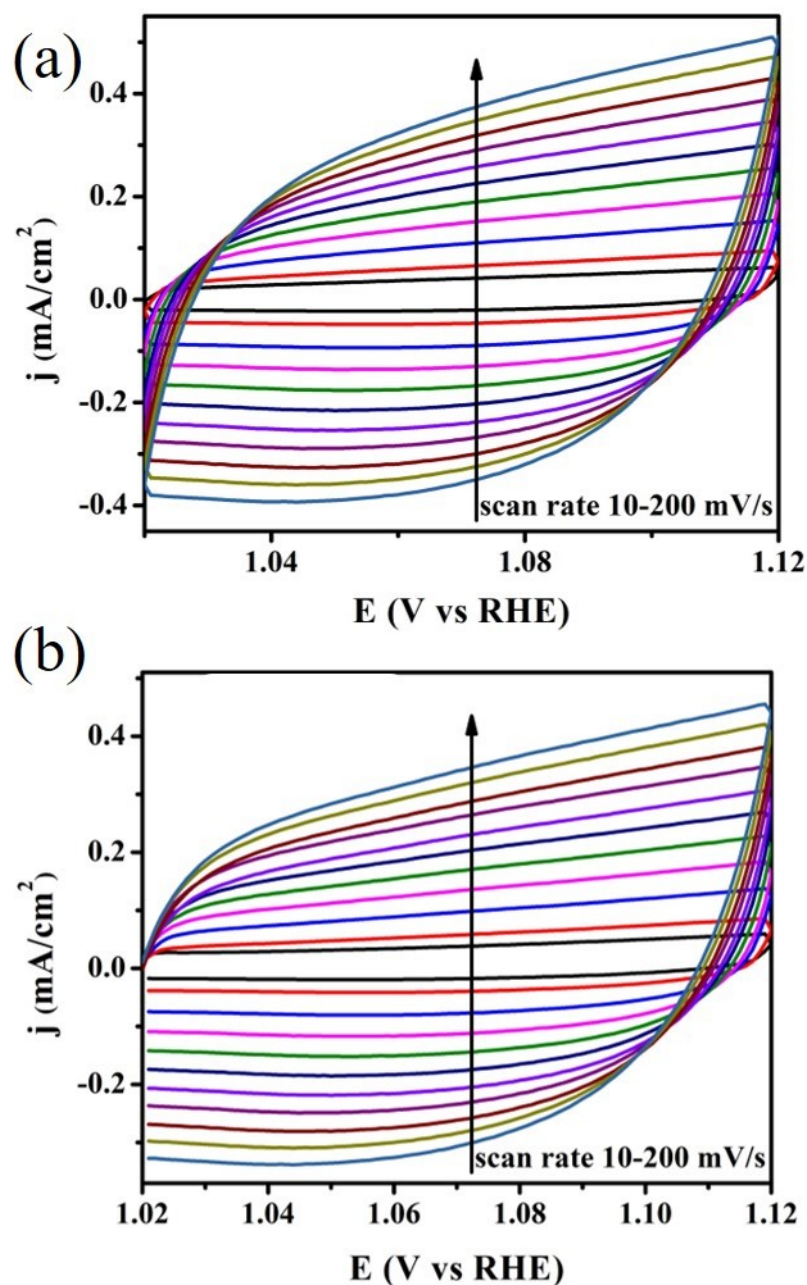


Figure S7. Double layer capacitance and capacitive currents as a functional of scan rate.

References

- 1 S. Zhao, Y. Wang, J. Dong, C.-T. He, H. Yin, P. An, K. Zhao, X. Zhang, C. Gao, L. Zhang, J. Lv, J. Wang, J. Zhang, A. M. Khattak, N. A. Khan, Z. Wei, J. Zhang, S. Liu, H. Zhao and Z. Tang, *Nat Energy*, 2016, **1**, 16184.
- 2 X. Cai, F. Peng, X. Luo, X. Ye, J. Zhou, X. Lang and M. Shi, *ChemSusChem*, 2021, **14**, 3163–3173.
- 3 X. Wang, H. Zhang, Z. Yang, C. Zhang and S. Liu, *Ultrasonics Sonochemistry*, 2019, **59**, 104714.
- 4 Z. Xue, K. Liu, Q. Liu, Y. Li, M. Li, C. Y. Su, N. Ogiwara, H. Kobayashi, H. Kitagawa, M. Liu and G. Li, *Nature communications*, 2019, **10**, 5048
- 5 L. Zhao, B. Dong, S. Li, L. Zhou, L. Lai, Z. Wang, S. Zhao, M. Han, K. Gao, M. Lu, X. Xie, B. Chen, Z. Liu, X. Wang, H. Zhang, H. Li, J. Liu, H. Zhang, X. Huang and W. Huang, *ACS Nano*, 2017, **11**, 5800–5807.
- 6 Q. Zha, F. Yuan, G. Qin and Y. Ni, *Inorg Chem*, 2020, **59**, 1295–1305.
- 7 J. Jiang, L. Huang, X. Liu and L. Ai, *ACS Appl Mater Interfaces*, 2017, **9**, 7193–7201.
- 8 X. Zhang, W. Sun, H. Du, R. M. Kong and F. Qu, *Inorg Chem Front*, 2018, **5**, 344–347.
- 9 X. F. Lu, P. Q. Liao, J. W. Wang, J. X. Wu, X. W. Chen, C. T. He, J. P. Zhang, G. R. Li and X. M. Chen, *J Am Chem Soc*, 2016, **138**, 8336–8339.
- 10 T. Fan, F. Yin, H. Wang, X. He and G. Li, *Int J Hydrogen Energy*, 2017, **42**, 17376–17385.
- 11 Y. Fang, X. Li, F. Li, X. Lin, M. Tian, X. Long, X. An, Y. Fu, J. Jin and J. Ma, *J Power Sources*, 2016, **326**, 50–59.
- 12 G. Arunkumar, P. Nantheeswaran, M. Mariappan, R. K. Kamlekar, M. Pannipara, A. G. Al-Shehmi and S. P. Anthony, *New Journal of Chemistry*, 2023, **47**, 9654–9660.